Available online at www.sciencedirect.com
ScienceDirect
Catalysis Today 129 (2007) 428–434
CATALYSIS TODAY
www.elsevier.com/locate/cattod

Hydrogen evolution by water splitting using novel composite zeolite-based photocatalyst

Nidhi Dubey, Nitin K. Labhsetwar, Sukumar Devotta, Sadhana S. Rayalu *

Environmental Materials Unit, National Environmental Engineering Research Institute (NEERI), Nagpur 440020, India

Available online 21 September 2007

Abstract

Novel zeolite-based material showing photocatalytic properties in the visible light have been synthesized by incorporating TiO_2, heteropolyacid (HPA) and transition metal, namely cobalt. This material shows high efficiency for water splitting under visible light irradiation. Hydrogen generation to the tune of 2171 μmol/h/g of TiO_2 has been achieved for the composite photocatalyst synthesized as compared to H_2 evolution rate to the tune of 131.6 μmol/h/g of TiO_2 for Degussa P25. This suggests that the TiO_2 which gets effectively dispersed and stabilized on the surface of zeolite works synergistically with cobalt and heteropolyacid to make the material active in visible light for evolution of hydrogen from water. TiO_2 is the photocatalyst, HPA functions as the dye sensitiser as well as redox system; zeolite functions as support matrix and as electron acceptor in synergy with cobalt. The probable mechanism for improved hydrogen evolution rate using such composite photocatalyst has been discussed.

Keywords: Hydrogen; Water splitting; Visible light; Zeolite-based photocatalyst

1. Introduction

Hydrogen is one of the most important chemicals in the industry. It is considered as the fuel for future and can be produced from plentiful and green source, namely water. Photochemical hydrogen generation via splitting of water to molecular hydrogen and oxygen by visible light (reaction (1)) is the first step for artificial photosynthesis reaction. In the subsequent steps of photosynthesis, the reduction of CO_2 to higher reduced products like formaldehyde, methanol and carbohydrates occurs.

$$H_2O \xrightarrow{h\nu} H_2 + \tfrac{1}{2}O_2 \quad (1)$$

The energy storage capacity of H_2 per gram (119,000 J/g) is very high as compared to that for oil. It is three times higher than the storage capacity of oil (40,000 J/g). The water splitting process for hydrogen generation has two major advantages, namely the raw material is abundant and cheap and, the combustion of H_2 in air (reverse of reaction (1)) produces water. This makes the whole process cyclic and non-polluting. Only 5% of the commercial hydrogen is produced by water electrolysis, while other 95% hydrogen is mainly derived from fossil fuels [1]. Fujishima and Honda have reported electrochemical hydrogen production using TiO_2 [2]. Since then extensive research is going on all over the world in search of materials that can photocatalyse water splitting reaction. In water splitting reaction H_2 is generated on the CB and oxygen on the VB. In order to make photocatalytic water splitting a feasible and economically viable process it is essential to use such an energy source which is not only green but is also cheap and available in abundance. Sunlight appears to be the most suitable option. However, in the solar spectrum the ultraviolet portion is 5% and the rest is contributed mainly by visible and infrared portion. Thus, for maximum utilization of sunlight, it is required to develop such material that can take up visible light. A major drawback associated with semiconductor mediated photocatalysis reactions is back electron transfer, which results in recombination of electron hole pair. This is the reason for poor efficiency of these reactions. When the semiconductor is supported on a zeolite matrix, the structural properties of the zeolite delay this back electron transfer and enable generation of long lived charged species [3]. Many supported photocatalysts have been reported for water splitting in visible light. Sathish et al. reported preparation of cadmium sulphide

* Corresponding author. Tel.: +91 712 2247828; fax: +91 712 2249900.
E-mail address: s_rayalu@neeri.res.in (S.S. Rayalu).

0920-5861/$ – see front matter © 2007 Elsevier B.V. All rights reserved.
doi:10.1016/j.cattod.2006.09.041

nanoparticles (6–12 nm) by a precipitation process using different zeolite matrices as templates. This photocatalyst is visibly active and was used for hydrogen evolution from water [4]. Dutta and Vaidyalingam reported the photocatalytic activity of RuO_2/zeolite Y for H_2 evolution from H_2O using the system $Ru(bpy)_3^{2+}$, Na_2 EDTA and methyl viologen (MV^{2+}) [5]. Guan et al. reported the photocatalytic activity of a CdS/ETS-4 composite for hydrogen production from water under visible light irradiation (wavelength >420 nm) [6]. Domen and co-workers reported that chemical fixation of xanthene dyes on platinized TiO_2 particles via silane coupling reagent resulted in photocatalyst system like Eosin Y fixed Pt-TiO_2 (EY-TiO_2) [7] with hydrogen evolution rate of 1166 μmol/h/g catalyst. Visibly active alumina supported cadmium sulphide photocatalyst was reported by Sinha et al. This photocatalyst was prepared for the photocatalytic reduction of water to generate hydrogen to the tune of 180.8 μmol/h/g CdS was reported using visible light [8].

Zeolites are crystalline aluminosilcates, which offer large surface area. The condensation effect and specific channel systems of the zeolites make such materials the most promising candidate for useful and highly reactive photocatalysts [9]. The high surface area and nanoscaled porous structure of zeolites enables incorporation of molecular entities like semiconductors TiO_2 [10,11] and heteropolyacids. Semiconductor-incorporated zeolites have gained importance as potential photocatalysts. The net negative charge on the aluminosilicate framework of zeolite is balanced by the counterions like Na^+, K^+ and other alkali and alkaline earth metals. These counterions present in the pores of zeolites play a very important role in the introduction of photocatalytic property. These counterions can be easily exchanged with transition metal ions like Co^{2+}. The presence of vacant d-orbitals in the transition metals makes them efficient redox catalyst and also the color of these ions enables them to work as chromophore that can absorb light radiations in the visible range. In addition, the heteropolyacids, which are supported on the surface of zeolite, have a tendency to be reduced to heteropolyblue (HPB), which takes up visible light. In the present study, the efficiency of the photocatalyst is evaluated by photoreduction of methyl orange to hydrazine and has been subsequently tested for hydrogen evolution.

2. Materials and methods

Following chemicals were used in the present synthesis; Commercial zeolite-Y (Tricat Germany), Degussa P25 TiO_2, titanium isopropoxide (Acros Organics), isopropanol (E-Merck), phosphomolybdic acid (E-Merck), Ethanol (E-Merck), and Cobaltous chloride (E-Merck). All chemicals were of AR grade and were used as such without further purification.

2.1. Synthesis of photocatalysts

For the synthesis of these composite metallozeolites, zeolite-Y (Si/Al = 2.5) is used as the base material.

2.1.1. Zeolite-Y/TiO_2

Five gram of commercial zeolite-Y was taken and 1.779 g of titanium isopropoxide was added to it drop wise. This mixture was homogenized and was calcined at 500 °C for 1 h. The dried calcined mass was then allowed to cool and it was then homogenized in a mixer.

2.1.2. Zeolite-Y/TiO_2/HPA

Incorporation of HPA. A 0.5 g of phosphomolybdic acid (HPA) was dissolved in 10 ml double distilled water. Five gram of zeolite-Y/TiO_2 was added to this solution. The slurry was stirred with a glass rod and dried at 70–80 °C on a hot plate. This was then ground to obtain a homogeneous mixture. This material is designated as zeolite-Y/TiO_2/HPA.

To highlight the role of zeolite following composite materials were synthesized to be used as blanks in specific without zeolite.

2.1.3. Co-P25

This composite was synthesized by impregnation of $CoCl_2{\cdot}6H_2O$ on P25 TiO_2. The details are published elsewhere [12].

2.1.4. HPA-P25

This composite was synthesized by impregnation of phosphomolybdic acid on P25 TiO_2. The details are published elsewhere [12].

2.1.5. Co-HPA-P25

This composite is synthesized by impregnation of $CoCl_2{\cdot}6H_2O$ and phosphomolybdic acid on P25 TiO_2. The details are published elsewhere [12].

2.1.6. Synthesis of zeolite-Y based photocatalytic material using titanium isopropoxide dissolved in isopropanol

Five gram of commercial zeolite-Y was taken and 1.779 g of titanium isopropoxide dissolved in 30 ml isopropanol was added to it drop wise. This mixture was thoroughly homogenized to avoid any lump formation and then the isopropanol was evaporated at 60–70 °C. The homogenized mixture was calcined in furnace at 500 °C for 1 h. After cooling, the calcined solid was dispersed in 100 ml double distilled water and its pH adjusted to 6.5. This was referred to as Slurry A. Solution B of cobalt chloride containing 0.2319 g $CoCl_2{\cdot}6H_2O$ was dissolved in 250 ml double distilled water to give metal exchanged zeolite corresponding to 5% of the calcium binding capacity (CBC) of zeolite-Y. Slurry A and Solution B were then mixed and stirred for 40 min on a magnetic stirrer. The catalyst was filtered and dried at 60 ± 5 °C. In this synthesis after exchange of Co^{2+} high temperature calcination is avoided since it may lead to formation of oxide of cobalt. The dried catalyst was impregnated with a solution of HPA containing 0.5 g HPA (10%, w/w) dissolved in 10 ml of double distilled water and the slurry was dried at 60 ± 5 °C and finally homogenized in a mixer. This catalyst was designated as PC-1.

2.1.7. Synthesis of USY based photocatalytic material

The synthesis of this material was conducted in the exactly similar manner as reported above but instead of zeolite-Y, US-Y (Si/Al = 80) is used. This is designated as PC-2.

2.1.8. Synthesis of β zeolite based photocatalytic material

The synthesis of this material was conducted in the exactly similar manner as reported above but instead of zeolite-Y, beta zeolite (Si/Al = 15) was used. This is designated as PC-3.

The materials PC-2 and PC-3 are synthesized in order to know the effect of pore size, Si/Al ratio and surface area of the support on the photocatalytic efficiency of the material.

2.2. Characterization of photocatalytic materials

X-ray diffraction studies of the synthesized photocatalyst were conducted to identify the appearance of TiO_2 phase on zeolite and to assess any effect on the crystallinity of zeolite during catalyst preparation. Philips Analytical Xpert diffractometer with monochromated Cu Kα radiation (λ = 1.54 Å) was used to record the X-ray diffraction of the synthesized materials. The samples were analyzed in a 2θ range of 10–60°. The *d*-spacing values for the synthesized materials are compared with the *d*-spacing values of most intense peaks of zeolite-Y and TiO_2. The XRD pattern is given in Fig. 1.

2.2.1. UV–vis-diffuse reflectance (UV-DRS)

Diffuse reflectance UV–vis spectra of the synthesized photocatalysts were recorded using a JASCO Spectrometer equipped with an integrating sphere. $BaSO_4$ was used as a reference material. The spectra are represented in Fig. 2.

2.2.2. Elemental analysis

Elemental analysis of the photocatalytic materials was carried out using Perkin-Elmer ICP-OES 4100 BV to assess the content of cobalt and molybdenum present.

2.2.3. Titanium estimation

Estimation of titanium in the samples was carried out using spectrophotometric method of analysis [13]. TiO_2 was converted into titanyl sulphate by digestion of the material with conc. H_2SO_4. Three percent H_2O_2 solution was added to it that resulted in the development of a yellow-orange color that was monitored spectrophotometrically at 410 nm.

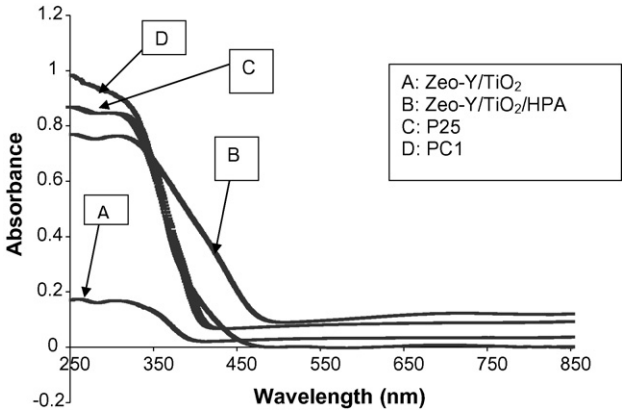

Fig. 2. UV–vis-diffuse reflectance spectra of the synthesized materials.

2.2.4. BET surface area analysis

The total surface area of the synthesized photocatalysts was calculated using BET Surface Area Analyser of make 'Micrometics': ASAP-2000 from JNARDDC, Nagpur. The surface area analysis in case of zeolite-based materials is important as it helps in understanding the location of different entities, whether they are within the pores or on the external surface.

2.3. Evaluation of the photocatalytic materials for methyl orange (MO) photoreduction

To test the photoreduction ability of the synthesized photocatalyst they were subjected to methyl orange photoreduction studies using the procedure described below.

The reactor used is made up of borosilicate glass. Dilute solution of methyl orange (5 mg/l) prepared in ethanol–double distilled water mixture (1:40) was taken to which a known amount of photocatalyst (75 mg) was added. The reaction mixture was stirred continuously to keep the catalyst in suspension during the reaction period. A water condenser was fitted to the reactor to prevent evaporative losses. The reaction mixture was illuminated with two 200 W Tungsten lamps for 4 h. After the end of the illumination period, the reaction mixture was subjected to ultra-centrifugation followed by filtration through cellulose nitrate membrane to get a clear solution. This solution was then analyzed spectrophotometrically at λ_{max} 464 nm to determine the extent of reduction of methyl orange. A catalyst blank, similar to the above reaction system was also simultaneously run without the addition of

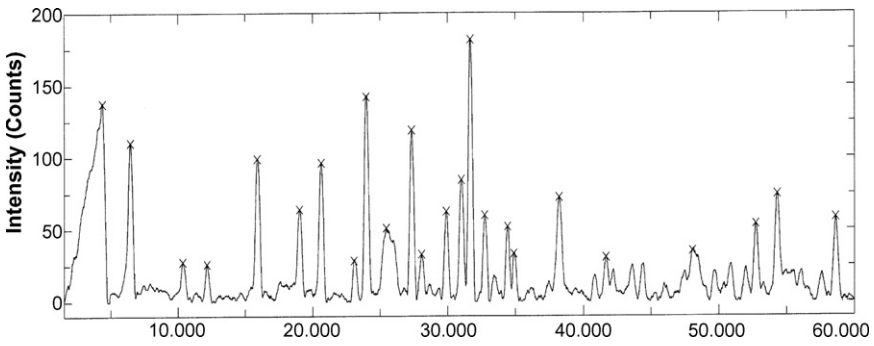

Fig. 1. XRD pattern of PC-1.

Table 1
Elemental analysis for various materials

Catalyst	Cobalt (mg/g)	Molybdenum (mg/g)	Theoretical TiO_2 (mg/g catalyst)	Obtained TiO_2 (mg/g catalyst)
Zeolite-Y/TiO_2	0.00	0.00	91	89.8
Zeolite-Y/TiO_2/HPA	0.00	48.28	83	82.75
PC-1	12.33	42.69	83	82.53
PC-2	5.61	41.63	83	80.27
PC-3	5.11	40.07	83	79.14

catalyst to account for the bleaching effect. Illumination blank consisted of a system similar to the reaction system; the only difference being that it was kept in dark to account for the adsorption effect. The photoreduction of methyl orange was estimated by calculating the difference in absorbance of working solution of methyl orange and the absorbance of the system subjected to illumination. The factors corresponding to adsorption of methyl orange on the zeolite surface and that due to bleaching were taken into account while calculating the difference in absorbance of the working methyl orange solution and the final methyl orange solution.

2.4. Water splitting experiment

A similar reactor as for the above reaction is used for carrying photoreducton of water to H_2. Ten millilitre of boiled double distilled water was taken and 75 mg of the catalyst was added to this. A 0.5 ml of ethanol was added as sacrificial electron donor to facilitate photoreduction. The reactor was equipped with a water condenser on the top of which was attached a gas collector to collect the evolved gas. The reactor was evacuated to ensure that the air in the headspace above the reaction mixture is removed. The reaction solution was continuously stirred to keep the catalyst in a homogenous suspension. The reactor is illuminated with two tungsten filament bulbs of 200 W each. Since the reactor is made up of borosilicate glass, no UV filter was used. In addition, no separate IR filter was used as the reactant water itself acted as the filter. The temperature of the reactants reached around 70 °C, as in the case of natural photosynthetic systems where splitting of water occurs in presence of light [14]. The reaction was carried out for several hours after which the gas collector was closed tightly and detached from the reactor. The gas collected in it was analyzed using GC/TCD equipped with a Molecular Sieve 5A column. The activity of the photocatalysts was compared with that of P25 TiO_2.

3. Results and discussions

3.1. Catalyst characterization

3.1.1. X-ray diffraction

In the synthesized photocatalyst the incorporation of the various elements during the synthesis procedure has no adverse effect on the crystallinity of the zeolite as can be seen from Fig. 1. The *d*-spacing values for the most prominent peaks of the anatase phase TiO_2 are 3.52, 1.88 and 1.7 Å. The formation of anatase phase can be seen in XRD pattern of all the photocatalysts, however, these peaks are not very prominent because it is highly dispersed in the zeolite matrix [15]. Also no change in the unit cell dimension was observed after calcinations of titanium isopropoxide on the zeolite surface.

3.1.2. UV–vis-diffuse reflectance spectra

The UV–vis-diffuse reflectance plots of the catalysts are represented in Fig. 2. In the spectra there is a characteristic peak of TiO_2 with a prominent red shift when compared with the spectra of P25 TiO_2. This is due to the incorporation of Co^{2+} and HPA into the zeolite, which has a remarkable influence on the light absorption property of TiO_2. The synergistic effect of Co^{2+} and HPA causes a red shift in the absorption band of TiO_2. Apart from the red shift there is also seen an absorbance in the visible region around 521 nm, which can be a possible reason for high activity of PC-1 in the visible region.

3.1.3. Elemental analysis

Elemental analysis conducted for evaluating the content of cobalt and molybdenum into the zeolite matrix shows that the experimental values closely agree with the theoretically calculated values. The results pertaining to TiO_2 estimation also show the same trend as seen from Table 1. It is seen that almost negligible amount of TiO_2 was leached during the 4 h leaching experiment. This shows that the anchoring of TiO_2 is very firm on the zeolite surface. The deposition of TiO_2 on the external surface of zeolite does not hinder the entry of the Co^{2+} within the pores of zeolite since the size of Co^{2+} is very small (0.745 Å) as compared to the window size of zeolite-Y, which is 7.4 Å. The content of molybdenum also agrees well with the targeted loading of HPA.

3.1.4. BET surface area analysis

The BET surface area of the metallozeolite photocatalysts has been determined and is represented in Table 2. The surface area of the photocatalysts decreases as we incorporated

Table 2
BET Surface Area of the synthesized metallozeolites

Catalyst	BET surface area (m^2/g)
Zeolite-Y	764.81
US-Y	727.70
Beta zeolite	466.20
Zeolite-Y/TiO_2	706.08
Zeolite-Y/TiO_2/HPA	643.05
PC-1	557.64
PC-2	559.17
PC-3	406.38

different entities in the zeolites. In zeolites, maximum surface area is within the pores. The decrease in surface area with incorporation of TiO_2 in the impregnated form zeolite-Y/TiO_2 is not very pronounced. Similar trend has been observed for zeolite-Y/TiO_2/HPA. This is because in impregnation technique, the entities TiO_2 and HPA are present on the external surface and not in the pores; therefore the reduction in surface area is not much. Since the size of HPA molecule is 10 Å, which is more than the pore opening of zeolite-Y (7.4 Å) the HPA molecule is impregnated on the external surface only and not within the pores. This is quite evident from the BET surface area data presented in Table 2. However, in case of photocatalysts PC-1–PC-3 we find that the decrease in surface area is prominent. This is because in these photocatalysts the transition metal ion Co^{2+} are incorporated within the pores and not on the external surface. These transition metal ions occupy surface area within the pores and hence a decrease is observed.

3.2. Methyl orange photoreduction

Photoreduction of methyl orange to the tune of 4.7 mg/gTiO_2 was obtained for the catalyst PC-1. As compared to photocatalysts zeolite-Y/TiO_2 and zeolite-Y/TiO_2/HPA, the performance of PC-1 is far better as seen from Fig. 3. The results for blanks Co-P25, HPA-P25 and Co-HPA-P25 have been reported in detail elsewhere [12].

3.3. Water splitting

The results presenting the amount of hydrogen generated in μmol/h/g of TiO_2 are given in Fig. 4. From the figure, it is seen that the zeolite-based synthesized photocatalyst PC-1 gives a yield of 2171 μmol/h/g TiO_2 (180 μmol/h/g catalyst). This value is quite high as compared to the values reported for other visibly active photocatalysts, viz.; CdS/ETS-4 that gives 175 μmol H_2/h/g catalyst [6] and Pt and CdS clusters in zeolite-Y [16] that gives 691.9 μmol H_2/h/g CdS. The heteropolyacid encapsulated TiHY zeolite [17] gives 0.6 μmol H_2/h/g catalyst in contrast to the H_2 evolution rate

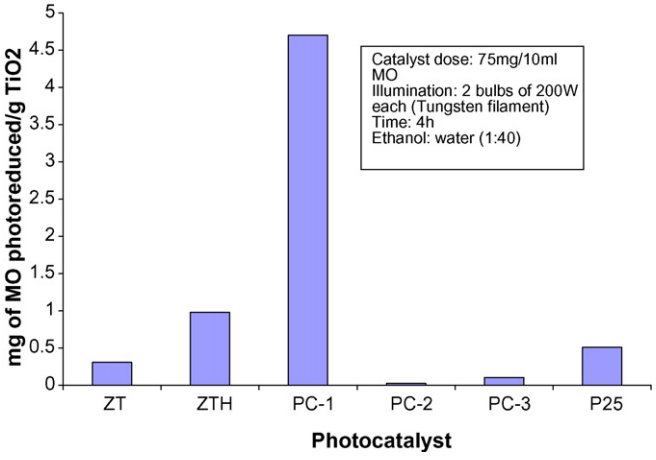

Fig. 3. Photoreduction of methyl orange using different photocatalysts, ZT = Zeolite-Y/TiO_2, ZTH = Zeolite-Y/TiO_2/HPA.

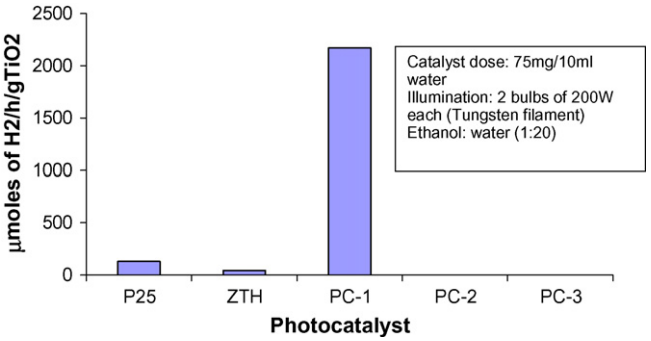

Fig. 4. Photoreduction of water to evolve hydrogen using different photocatalysts.

of 2171 μmol/h/g TiO_2 for PC-1 sample reported in this work. This may be attributed to incorporation of Co^{2+} ion-by-ion exchange in the pores of zeolite and TiO_2 by impregnation route on the surface of zeolite as compare to heteropolyacid encapsulated TiHY zeolite in which TiO_2 is incorporated in the pores via the ion exchange route. The incorporation of TiO_2 via impregnation occurs on the external surface of zeolite. Thus, there is no formation of nanoparticles (which normally occurs in the pores). The H_2 yield in case of P25 TiO_2 was 131.6 μmol/h/gTiO_2. To the best of our knowledge, zeolite-based photocatalyst is performing better than most of the TiO_2 based catalyst reported in literature so far. Dye sensitized composite photocatalyst reported by Domen and co-workers, namely Eosin-Y fixed Pt-TiO_2 catalyst shows H_2 evolution rate of 1166 μmol/h/g catalyst [7]. This clearly indicates that the synergistic effect of Co^{2+} and HPA with TiO_2 supported on zeolite has a remarkable effect on the hydrogen yield. Ethanol which is added to the water plays an important role in photoreduction. In this experiment the ratio of ethanol:water is 1:20. Experiments with 1:10 and 1:1 ratio of ethanol:water did not show any increase in hydrogen generation showing that the ethanol acts only for facilitating water splitting and does not contribute to the hydrogen yield. However, with 1:40 ethanol:water mixture the yield of hydrogen was less than that obtained for 1:20. Thus, the ratio of ethanol-water mixture was optimized for the water splitting experiment.

3.4. Effect of zeolite matrix

The high surface area of zeolite provides sites for homogenous dispersion of TiO_2. By virtue of its highly porous structure and ion exchange capacity, zeolites prove to be very efficient in incorporating transition metal ions which are very good catalysts. The zeolite-Y structure also possesses acid and basic sites and can accept as well as donate electrons. Different composites without zeolite were synthesized as well in order to highlight the role of zeolite not only as a support for stabilizing different species but also as an active component in enhancing the overall efficiency of the synthesized material. The following composites: Co-P25, HPA-P25, and Co-HPA-P25 were evaluated for methyl orange photoreduction. The experimental protocol and results pertaining to the comparative studies of the zeolite-based

photocatalyst for MO photoreduction and these blanks are reported previously by the authors [12]. It therefore appears that the zeolite matrix has a considerable role in delaying the recombination of holes and electrons of the semiconductor TiO_2. This is because the electrons hop from one acid site to another and thus delays the recombination of electrons ands holes. In case of ultra-stable zeolite Y (Si/Al = 80) and beta zeolite (Si/Al = 15) the aluminium content is very low as compared to that of NaY (Si/Al = 2.5) zeolite. Lesser number of Al^{3+} sites have a lesser tendency than zeolite-Y to delay this electron hole recombination. Therefore, the electron transfer mechanism is not enhanced by this zeolite and US-Y. This is reflected in the negligible photoreduction efficiency of the photocatalysts PC-2 and PC-3 in terms of methyl orange photoreduction (Fig. 3) and H_2 evolution (Fig. 4) based on these support matrices.

3.5. Effect of cobalt and HPA

The MO photoreduction of the materials synthesized by supporting TiO_2 on zeolite (zeolite-Y/TiO_2) are much low as compared to zeolite-Y/TiO_2/HPA and PC-1 (Fig. 3). These results are very crucial as they highlight the role of cobalt and HPA in enhancing photoreduction in the visible range. As seen from Fig. 2 the synthesized photocatalyst (PC-1) shows much more absorbance in the visible range as compared to P25. Co^{2+} which is a colored ion acts as chromophore and absorbs visible light. The presence of vacant d-orbitals in Co^{2+} act as electron trap and prevent their recombination with the holes in the valence band of TiO_2. Since the reduction potential of Co^{2+}/Co is −0.27 V at 25 °C [18] and that of TiO_2 CB is −0.52 V, the transfer of electrons takes place from the CB of TiO_2 to the Co^{2+} via the zeolite framework. The HPA incorporated on the high surface area offered by zeolites work in synergism with Co^{2+} to make the material visibly active. Anandan and Yoon [17] have reported that the electron released by TiO_2 is accepted by the excited HPA species that is reduced to heteropolyblue (HPB). This heteropolyblue (HPB) absorbs light in the visible range and hence enables the photocatalytic water splitting under visible light irradiation. In addition, the redox property of HPA is further helpful in facilitating photoreduction because the reduced HPA (HPB) can release its electron to the water molecule to reduce it to evolve hydrogen. In case of the synthesized photocatalyst PC-1, Co^{2+} is also present in addition to HPA. Due to this, there is further enhancement in visible light absorption. In addition, the tendency of Co^{2+} and HPA to facilitate reduction reaction enhances the efficiency of PC-1. The yield of H_2 is 2171 μmol/h/g TiO_2 as compared to 131.6 μmol/h/g TiO_2 in case of P25 TiO_2. As already discussed in previous section the H_2 evolution rate has improved significantly as compared to other zeolite-based composite photocatalyst [17]. This highlights the role of Co^{2+} ions, which assist in facilitating electron transfer reaction. The optimized content of Co^{2+} was 5% CBC of zeolite for exchange [19] and the optimized loading of HPA was 10% (w/w) [19].

3.6. Summary of proposed mechanism

The mechanism of photoreduction proposed here is in line with that proposed by Anandan and Yoon [17]. By absorbing light TiO_2 generates an electron rich centre in the conduction band and a hole in the valence band. The HPA present on the surface of zeolite takes up the electron from the CB. This is because the potential of the CB of TiO_2 is −0.52 V and that of HPA is −0.28 V. By taking up the electron from the CB of TiO_2, HPA is reduced to heteropolyblue (HPB). This HPB can absorb light in the visible range (at around 700 nm). The electron from HPB then is transferred to Co^{2+} ions present in the pores of zeolite via the zeolite framework by a hopping mechanism [20]. The zeolite has a negatively charged microenvironment. The negative charge is counterbalanced by the cations. Beer et al. have proposed a mechanism in which the electron moves from one Lewis acid site (Al^{3+}) to the other. This jumping or hopping of electron from one Al^{3+} to the other brings about a delay in the electron hole recombination reaction. The Co^{2+} ion transfers the electron to water that is reduced to hydrogen. The HPB after releasing the electron to Co^{2+} is oxidised to HPA. By virtue of light absorption properties, HPA absorbs light and gets excited to HPA*. This excited HPA takes up electron from the electron donor and is reduced to HPB. Thus, the formation of HPB occurs via two routes. This HPB releases its electron to Co^{2+} to reduce water in the same way as discussed above.

The zeolite framework and Co^{2+} have a vital role in delaying electron hole recombination reaction. Semiconductor mediated photocatalytic reactions have a low efficiency due to the back electron transfer reaction. The presence of acid and basic sites on the zeolite helps in delaying the recombination reaction. The synthesized composite photocatalysts is thus showing far better efficiency (2171 μmol/h/g TiO_2) as compared to the bulk TiO_2 (131.6 μmol/h/g TiO_2) for photoreduction of water to produce hydrogen. This reduction of water to hydrogen follows the Z-scheme mechanism for water splitting in plants as reported by Anandan and Yoon [17]. The zeolite helps to stabilize TiO_2 and HPA, which then act in synergy with the Co^{2+} present in the exchanged form in the zeolitic cavities to enable the material to work for photoreduction of water under visible light. Further studies are in progress to substantiate these mechanistic aspects.

4. Conclusion

The synthesized composite photocatalyst having a combination of TiO_2, Co^{2+} and HPA shows a higher efficiency for photo reduction of water to hydrogen in the visible light range as compared to the unsupported semiconductor photocatalyst TiO_2. The role of zeolite in this composite photocatalyst is not only to provide a high surface area and ion exchange properties for incorporation of TiO_2, HPA and Co^{2+} but also it serves as an electron acceptor which delays the back electron transfer reaction to promote photoreduction of water to hydrogen. Co^{2+} not only enhance the visible light absorption property of the material but also enhance its photocatalytic efficiency. The

present work is just an initial step towards hydrogen production from a clean and green source. Further steps for improving the efficiency of the reaction are in progress in our laboratory. This paper discusses photocatalyst with TiO_2 and HPA supported on zeolite external surface with Co^{2+} in the pores. Efforts are in progress to design photocatalyst by incorporating TiO_2 in pores and HPA on surface and vice versa.

Acknowledgements

This work was carried out under the Department of Science & Technology, Government of India, the MITSUI Environmental Engineering Trust (MEET) sponsored project No. G-5-1148 and CSIR Network Project No. CORE-08 (1.1). Thanks are also due to NCL Pune, JNARDDC Nagpur and Institute of Inorganic Chemistry, Academy of Sciences of the Czech Republic, Czech Republic for help in various evaluation and characterization studies.

References

[1] M. Ni, M.K.H. Leung, D.Y.C. Leung, K. Sumathy, Water electrolysis—a bridge between renewable resources and hydrogen, in: Proceedings of the International Hydrogen Energy forum, vol. 1, 25–28 May, Beijing, PR China, (2004), pp. 475–480.
[2] A. Fujishima, K. Honda, Nature 238 (1972) 37–38.
[3] S.K. Das, P.K. Dutta, Microporous Mesoporous Mater. 22 (1998) 475–483.
[4] M. Sathish, B. Vishwanathan, R.P. Vishwanath, Int. J. Hydrogen Energy 31 (7) (2006) 891–898.
[5] P.K. Dutta, A.S. Vaidyalingam, Microporous Mesoporous Mater. 62 (2003) 107–120.
[6] G. Guan, T. Kida, K. Kusakabe, K. Kimura, X. Fang, T. Ma, E. Abe, A. Yoshida, Chem. Phys. Lett. 385 (2004) 319–322.
[7] R. Abe, K. Hara, K. Sayama, K. Domen, H. Arakawa, J. Photochem. Photobiol. A: Chem. 137 (1) (2000) 63–69.
[8] A.S.K. Sinha, N. Sahu, M.K. Arora, S.N. Upadhyay, Catal. Today 69 (2001) 297–305.
[9] M. Matsuka, M. Anpo, J. Photochem. Photobiol. C: Photochem. Rev. 3 (2003) 225–252.
[10] S. Corrent, G. Cosa, J.C. Scaiano, M.S. Galletero, M. Alvaro, H. Gracia, Chem. Mater. 13 (2001) 715–722.
[11] S.H. Bossmann, C. Turro, C. Schnabel, M.R. Pokhrel, L.M. Payawan Jr., B. Baumeister, M. Worner, J. Phys. Chem. B 105 (23) (2001) 5374–5382.
[12] N. Dubey, S.S. Rayalu, N.K. Labhsetwar, R.R. Naidu, R. Chatti, S. Devotta, Appl. Catal. A: Gen. 303 (2) (2006) 152–157.
[13] P. Yue, F. Khan, Int. J. Hydrogen Energy 16 (9) (1991) 613–699.
[14] M. Zalas, M. Laniecki, Solar Energy Mater. Solar cells 89 (2–3) (2005) 287–296.
[15] S. Anandan, M. Yoon, J. Photochem. Photobiol. C: Photochem. Rev. 4 (2003) 5.
[16] Y.-J. Hwang, S.-J. Kim, S. Park, J.-H. Yang, H. Kim, J.-H. Choy, Bull. Korean Chem. Soc. 21 (2) (2000) 187–192.
[17] S. Anandan, M. Yoon, J. Photochem. Photobiol. A: Chem. 160 (2003) 181–184.
[18] J.D. Lee, Concise Inorganic Chemistry, 5th ed., John Wiley and Sons, (1996) p. 166.
[19] Data communicated elsewhere.
[20] R.V. Chatti, S.S. Rayalu, N. Dubey, N. Labhsetwar, S. Devotta, Solar Energy Mater. Solar Cells 91 (2007) 180.